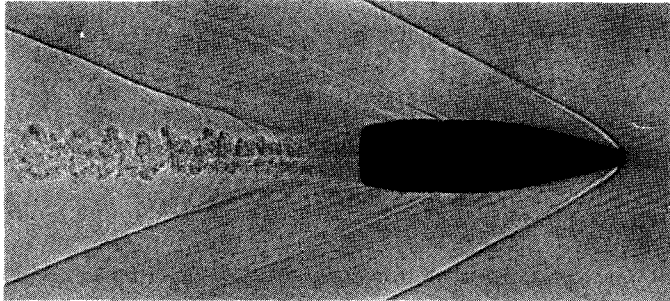


Battlefield Weapons Systems
& Technology, Volume X

MILITARY BALLISTICS



A Basic Manual

Contents

List of Illustrations	ix
Chapter 1 History of Ballistics	1
Chapter 2 Internal Ballistics - Part I	9
Internal Ballistics - Part II	39
Chapter 3 Intermediate Ballistics	53
Chapter 4 External Ballistics - Part I	71
External Ballistics - Part II	103
Chapter 5 Terminal Ballistics - Part I	137
Terminal Ballistics - Part II	153
Chapter 6 Wound Ballistics	161
Chapter 7 Ballistics Instrumentation	173
Answers to Self Test Questions	201
Bibliography	207
Index	209

List of Illustrations

Chapter 1

FIG 1.1	Ballista	2
---------	----------	---

Chapter 2 - Part I

FIG 2.1	The main ballistic components of the loaded gun	10
FIG 2.2	105 mm shell featuring a single driving band	11
FIG 2.3	7.62 x 51 mm cartridge together with a fired boattailed bullet and an unfired flat-based bullet	12
FIG 2.4	105 mm calibre APFSDS (Armour Piercing Fin-Stabilised Discarding Sabot) with sabot attached	12
FIG 2.5	Cross-section of a shotgun cartridge	13
FIG 2.6	Common shapes of propellant granules	14
FIG 2.7	Preparation of smokeless propellants	14
FIG 2.8	Three stages in the burning of a cylindrical propellant granule	15
FIG 2.9	Ignition temperature of smokeless propellants	15
FIG 2.10	Typical burning rate constants	16
FIG 2.11	Burning rate against pressure for a typical propellant	16
FIG 2.12	Pressure within a closed-vessel plotted against time	17
FIG 2.13	Typical adiabatic (closed-vessel) flame temperatures	18
FIG 2.14	Examples of ballistic size	18
FIG 2.15	Types of progressive granules	19
FIG 2.16	Cross-sections of 7 hole multi-tube granule	20
FIG 2.17	Examples of granule shapes and their form function coefficients	20

FIG 2. 18	Configuration of igniter and propellant charge in typical ammunition	21
FIG 2. 19	Typical pressure/time, velocity/time and travel/time curves	23
FIG 2. 20	Typical pressure/space and velocity/space curves	23
FIG 2. 21	The four factors which determine projectile acceleration	24
FIG 2. 22	Typical frictional force during firing	24
FIG 2. 23	The approximate distribution of liberated energy	25
FIG 2. 24	Approximate recoil energies relative to total available energy	25
FIG 2. 25	Examples of peak pressure	26
FIG 2. 26	Pressure/space curves for three full charges of propellant	28
FIG 2. 27	Erosion of the gun	29
FIG 2. 28	An eroded gun sectioned to show enlargement of the bore and worn rifling	30
FIG 2. 29	Cross-section of the bore and relative rates of erosion	31
FIG 2. 30	Rifling depth in a Probertised barrel	32
FIG 2. 31	Examples of practical barrel life	32
FIG 2. 32	Chieftain tank fitted with 120 mm lagged gun	33
FIG 2. 33	The principle of the recoilless jet reaction gun	34
FIG 2. 34	LAW 80 (early model) anti-tank recoilless rocket launcher (Photo by courtesy of Hunting Engineering Ltd)	34
FIG 2. 35	120 mm Combat recoilless jet reaction gun	34
Chapter 2 - Part II		
FIG 2. 36	Flow diagram for a lumped parameter computer model of internal ballistics, with description given on left hand side	50

Chapter 3

FIG 3. 1	Shock waves formed by the release of high pressure gas from a muzzle	55
FIG 3. 2	Shock wave formation before projectile exit	56
FIG 3. 3	The precursor blast field of a 5. 56 mm calibre rifle	56
FIG 3. 4	The initial formation of shock waves shortly after projectile exit	57
FIG 3. 5	Expansion of the blast field	58
FIG 3. 6	Final phase of the blast field before contraction of the bottle shock and Mach disc	58
FIG 3. 7	Preflash	59
FIG 3. 8	Flash	60
FIG 3. 9	The intense secondary flash of a 120 mm calibre Chieftain tank gun (Photo by courtesy of T. D. and P. W. Royal Armoured Corps, Bovington Camp)	60
FIG 3. 10	The intense secondary flash from the breech nozzle of a 120 mm calibre Wombat recoilless gun	61
FIG 3. 11	The primary and intermediate flash of a 7. 62 mm calibre rifle showing the total absence of secondary flash	61
FIG 3. 12	Conical, slotted tube and bar type flash suppressors on 5. 56 mm calibre rifles	62
FIG 3. 13	Cross-section of an idealised shock wave	63
FIG 3. 14	Table of overpressures in atmospheres against intensity of sound in decibels (reference pressure 2×10^{-5} Pascals)	64
FIG 3. 15	Methods of blast suppression	65
FIG 3. 16	9 mm calibre sten sub machine gun fitted with silencer	65
FIG 3. 17	The principle of the muzzle brake	67
FIG 3. 18	Muzzle brake fitted to British 105 mm calibre light gun	68

Chapter 4 - Part I

FIG 4.1	Motion of a projectile under no external influences	72
FIG 4.2	Motion of a projectile under the action of gravity	72
FIG 4.3	Compression waves at subsonic speed	73
FIG 4.4	Shock wave at supersonic speed	74
FIG 4.5	Shadowgraph of 7.62 mm bullet (Photo by courtesy of RMCS Shrivenham)	75
FIG 4.6	Shadowgraph of high drag training round (Photo by courtesy of RMCS Shrivenham)	75
FIG 4.7	Shadowgraph of space re-entry model showing detached shock wave	76
FIG 4.8	Base drag	77
FIG 4.9	Air resistance	78
FIG 4.10	Real and in-vacuo trajectories	79
FIG 4.11	The effect of air resistance on certain projectiles	80
FIG 4.12	Calibre radius head	81
FIG 4.13	Fractional calibre radius head	81
FIG 4.14	Boattail design	82
FIG 4.15	The variation of C_D with speed in the subsonic region for different nose shape projectiles	83
FIG 4.16	The variation of C_D with speed for two differently shaped projectiles	84
FIG 4.17	The variation of C_D with speed for a typical shell	84
FIG 4.18	The effect of base bleed on range	85
FIG 4.19	Angle of yaw	86
FIG 4.20	Over-turning moment	86
FIG 4.21	Stability of an arrow	87
FIG 4.22	British 81 mm mortar bomb (Photo by courtesy of RMCS Shrivenham)	88

List of Illustrations

xiii

FIG 4. 23	Gyroscopic motion	89
FIG 4. 24	Precession and nutation for a spinning projectile	89
FIG 4. 25	Over-stabilised shell	90
FIG 4. 26	Gyroscopic forces acting on a spinning top	91
FIG 4. 27	Rear view of spinning projectile : nose movement to the right	91
FIG 4. 28	Rear view of spinning projectile : nose movement downwards	92
FIG 4. 29	Rear view of spinning projectile : nose movement to the left	92
FIG 4. 30	Equilibrium yaw	93
FIG 4. 31	Magnus effect	93
FIG 4. 32	Variation of P , ρ , T and v with altitude	96
FIG 4. 33	Extension of range when firing eastward at low elevation	98
Chapter 4 - Part II		
FIG 4. 34	Parabolic motion in vacuo	104
FIG 4. 35	The effect of gravity and drag acting on a projectile	105
FIG 4. 36	Conservation of linear momentum	106
FIG 4. 37	Some exhaust velocities and specific impulses for various types of propellant	108
FIG 4. 38	Rocket trajectories	109
FIG 4. 39	Dynamic similarity	112
FIG 4. 40	The relationship between C_D and Re	113
FIG 4. 41	Viscous boundary layer	114
FIG 4. 42	Boundary layer separation	116
FIG 4. 43	Wind-axes	117
FIG 4. 44	Body-axes	118
FIG 4. 45	Variation of C_D with angle of yaw	119

FIG 4. 46	Variation of C_L with angle of yaw	119
FIG 4. 47	Variation of C_M with angle of yaw	120
FIG 4. 48	Spinning top	121
FIG 4. 49	Angular velocities of spinning top	122
FIG 4. 50	Resolved components of angular velocities	123
FIG 4. 51	Two arm model applied to spinning top	126
FIG 4. 52	Forces acting on a spinning shell	127
FIG 4. 53	Variation of C_M with M	128
FIG 4. 54	Two arm model applied to spinning projectile	129
FIG 4. 55	Typical patterns for aerodynamically stable projectiles	130
FIG 4. 56	Typical patterns for aerodynamically unstable projectiles	130
FIG 4. 57	Rosette motion	131
FIG 4. 58	Equilibrium yaw motion	131
FIG 4. 59	Increments of angular momentum	132
FIG 4. 60	Equilibrium yaw angle	133
Chapter 5		
FIG 5. 1	Angle of attack	138
FIG 5. 2	Impact of a long rod penetrator	141
FIG 5. 3	Perforation mechanisms	142
FIG 5. 4	Basic components of an APDS projectile	144
FIG 5. 5	Basic components of an APFSDS projectile	145
FIG 5. 6	Basic components of a HE fragmentation shell	145
FIG 5. 7	The shaped charge principle	147
FIG 5. 8	Penetrative performance of a conical liner	147
FIG 5. 9	Basic components of a HEAT projectile	148
FIG 5. 10	HEAT effect	149

List of Illustrations

xv

FIG 5. 11	Basic components for a HESH projectile	150
FIG 5. 12	HESH effect	150
Chapter 6		
FIG 6. 1	Wound track of subsonic projectile	162
FIG 6. 2	Stress wave formed by high velocity projectile	162
FIG 6. 3	Temporary cavity formed by high velocity projectile	163
FIG 6. 4	Selected stills from a high speed cine film showing the temporary cavitation (Photo by courtesy of CDE, Porton Down)	164
FIG 6. 5	The respective wounding effects of a soft bullet, unstable jacketed bullet and stable jacketed bullet	165
FIG 6. 6	The permanent record of cavitation effects as shown in standard soap blocks (Photo by courtesy of CDE, Porton Down)	165
FIG 6. 7	Possible cavitation effects with metallic armour	167
FIG 6. 8	The non-penetrating impact of a 9 mm bullet travelling at 330 m/s against 16 plys of Kevlar body armour (Photo by courtesy of CDE, Porton Down)	168
Chapter 7		
FIG 7. 1	Time scale for various illuminating sources	174
FIG 7. 2	A microflash photograph of a 105 mm shell in flight (Photo by courtesy of RMCS Shrivenham)	174
FIG 7. 3	A microflash photograph of 120 mm APDS in flight (Photo by courtesy of P. Fuller, RARDE)	175
FIG 7. 4	Experimental arrangement for spark photography	176
FIG 7. 5	Diagrammatic representation of the shadowgraph	176
FIG 7. 6	Multiple spark photograph (Photo by courtesy of P. Fuller, RARDE)	177
FIG 7. 7	Schlieren photograph of sphere (Photo by courtesy of P. Fuller, RARDE)	177

FIG 7. 8	The Schlieren system	178
FIG 7. 9	Rocket launching (Photo by courtesy of P. Fuller, RARDE)	179
FIG 7. 10	Compensation for film movement by rotating glass block	180
FIG 7. 11	Ballistic synchro technique (Diagram by courtesy of P. Fuller, RARDE)	181
FIG 7. 12	A ballistic synchro record of 120 mm APDS (Photo by courtesy of P. Fuller, RARDE)	181
FIG 7. 13	The rotating mirror streak camera (Diagram by courtesy of P. Fuller, RARDE)	182
FIG 7. 14	The rotating mirror framing camera (Diagram by courtesy of P. Fuller, RARDE)	182
FIG 7. 15	Image converter camera schematic	183
FIG 7. 16	Lead pellet impacting on hard target (Photo by courtesy of John Hadland Photographic Instrumentation Ltd., Herts, UK)	183
FIG 7. 17	Streak photograph of 7. 62 mm bullet travelling at approximately 840 m/s (Photo by courtesy of RMCS Shrivenham)	184
FIG 7. 18	X-ray shadowgraph of 0. 45 automatic during firing (Photo by courtesy of Hewlett Packard Ltd., Berks, UK)	184
FIG 7. 19	PCC equipment	186
FIG 7. 20	Principle of radio-doppler	187
FIG 7. 21	Principle of yaw sonde	188
FIG 7. 22	Principle of the 'V' cell	189
FIG 7. 23	Interpretation of pulse record	189
FIG 7. 24	Results from yaw sonde	190
FIG 7. 25	Shot position indicator (Photo by courtesy of M. S. Instruments Ltd., Kent, UK)	191
FIG 7. 26	Position of shock wave front	191
FIG 7. 27	Cartesian co-ordinate system	192

List of Illustrations

xvii

FIG 7. 28	Crusher gauge	193
FIG 7. 29	Basic interferometer system	195
FIG 7. 30	Direct optical method	196
FIG 7. 31	Bore-wire resistance method	196
FIG 7. 32	Linear displacement transducers	197